COMPONENT PART NOTICE

THIS PAPER IS A COMPONENT PART OF THE FOLLOWING COMPILATION REPORT: A

(TITLE): Characteristics of the Lower Atmosphere Influencing Radio Wave Propagation: Conference Proceedings of the Symposium of the Electromagnetic Wave Propagation Panel (33rd) Held at Spatind, Norway on 4-7 October 1983.

(SOURCE): Advisory Group for Aerospace Research and Development, Neuilly-sur-Seine (France).

TO ORDER THE COMPLETE COMPILATION REPORT USE AD-A145 046.

THE COMPONENT PART IS PROVIDED HERE TO ALLOW USERS ACCESS TO INDIVIDUALLY AUTHORED SECTIONS OF PROCEEDINGS, ANNALS, SYMPOSIA, ETC. HOWEVER, THE COMPONENT SHOULD BE CONSIDERED WITHIN THE CONTEXT OF THE OVERALL COMPILATION REPORT AND NOT AS A STAND-ALONE TECHNICAL REPORT.

THE FOLLOWING COMPONENT PART NUMBERS COMPRISE THE COMPILATION REPORT:

P003893

AD#:	TITLE:
AD-P003 885	Ice Depolarization on Low-Angle 11 GHz Satellite Downlinks.
AD-P003 886	The Effects of a Low-Altitude Nuclear Burst on Millimeter Wave Propagation.
AD-P003 887	Measurements of Atmospheric Effects on Satellite Links at Very Low Elevation Angle.
AD-P003 888	The Effects of Meterorology on Marine Aerosol and Optical and IR Propagation.
AD-P003 889	A System to Measure LOS (Line-of-Sight) Atmospheric Transmittance at 19 GHz.
AD-P003 890	A GaAs FET Microwave Refractometer for Tropospheric Studies.
AD-P003 891	Prediction of Multipath Fading on Terrestrial Microwave Links at Frequencies of 11 GHz and Greater.
AD-P003 892	Multipath Outage Performance of Digital Radio Receivers Using Finite-Tap Adaptive Equalizers.
AD-P003 893	Spherical Propagation Models for Multipath-Propagation Predictions.
AD-P003 894	Correcting Radio Astronomy interferometry Observations for Ionospheric Refraction.
AD-P003 895	The Estimation and Correction of Refractive Bending in the AR3-D Tactical Radar Systems.
AD-P003 896	Effect of Multiple Scattering on the Propagation of Light Beams in Dense Nonhomogeneous Media.
AD-P003 897	Adaptive Compensation for Atmospheric Turbulence Effects on Optival Propagation.
AD-P003 898	Effects of Atmospheric Turbulence on Optical Propagation.
AD-P003 899	A Radio Interference Model for Western Europe.
AD-P003 900	Transhorizon Microwave Propagation Measurements related to Surface Meteorological Parameters.
AD-P003 901	Tropospheric Propagation Assessment.

COMPONENT PART NOTICE (CON'T)

AD#:	TITLE:
AD-P003 902	Distortion of a Narrow Radio Beam in a Convective Medium.
AD-P003 903	Anomalous Propagation and Radar Coverage through Inhomogeneous Atmospheres.
AD-P003 904	The Prediction of Field Strength in the Frequency Range 30 - 1000 MHz.
AD-P003 905	VHF and UHF Propagation in the Canadian High Arctic.
AD-P003 906	Considerations Pertinent to Propagation Prediction Methods Applied to Airborne Microwave Equipments.

SPHERICAL PROPAGATION MODELS FOR MULTIPATH-PROPAGATION PREDICTIONS

by

L.P. Ligthart
Delft University of Technology
Dept. of Electrical Engineering
Mekelweg 4
2628 CD Delft

Summary

Multipath fading leads to a limitation in the availability and/or reliability of microwave links. To study the propagation mechanism under fading conditions propagation models based on ray theory, above a spherical earth have been developed and compared to the well-known planar propagation model above a "flattened earth". The reasons for studying spherical propagation models are a) to avoid the limitation of small elevation angles in planar propagation models, b) to investigate the computed and measured path delay on the microwave line of sight links, and c) to set up an analytical approach for the spherical propagation model without numerical difficulties and computing-time intensive procedures.

In this paper computational results of the models are shown, including an accuracy analysis, and the use of spherical propagation models is illustrated for surface duct layers above water.

1. Introduction

Multipath propagation can cause large variations in the received signal level. To prevent multipath fading on terrestrial microwave radio links two diversity techniques are frequently used:

- frequency-diversity,
- height-diversity.

Another possibility for multipath fading reduction is derived from the angle of arrival dependency of incoming rays at the receiver antenna. This third diversity technique looks promising when use is made of electronically controlled limited scan antennas (Ref. 1). Hybrid reflector antennas for multipath fading reduction have determined the German and the Dutch contribution to the COST 204 project (European Co-Operation in the field of Scientific and Technical Research-Commission of the European Communities). The project is entitled "Phased Array Antennas and their Novel Applications" (Ref. 2).

In The Netherlands the Dr. Neher Laboratory of the Dutch PTT and the Microwave Laboratory of the Delft University of Technology have collaborated on a research program to investigate the possibilities of using limited scan antennas on digital microwave line of sight links. To come up with antenna specifications for fading reduction, group delay requirements in two ray propagation models have been considered. Firstly, the planar propagation model has been used. This model approximates small elevation angles and can be found by an "earth flattening" coordinate transformation to preserve relative curvature between rays and the earth. Because accurate time delay information is needed for specifying the wanted antenna characteristics spherical models have also been investigated.

In Section 2 some attention is paid to ray parameters in planar and spherical models, assuming a constant refractive index gradient over a given height segment.

In Section 3 results of time delay computations for both models and of the accuracy analysis for the spherical model are shown.

In Section 4 a modified logarithmic refractive index profile is assumed in order to study the propagation mechanism through surface ducts above water under different spherical model conditions.

2. Ray parameters for planar and spherical models

In the model with planar earth (Figure 1) the vertical refractive index profile m is assumed to be dependent on z only and is characterized by the transformation

$$\frac{dn(r)}{dr} \approx \frac{dm(z)}{dz} - \frac{1}{R_a} = B'' - \frac{1}{R_a}$$

where n = refractive index in the spherical model with earth radius R_a and with assumed radial dependency r

n_o = refractive index in the planar model

B" = refractive index gradient per meter in the planar model

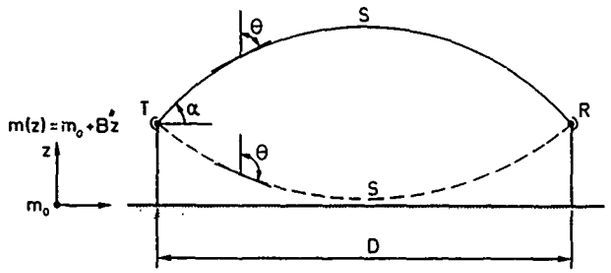

Figure 1. Planar propagation model

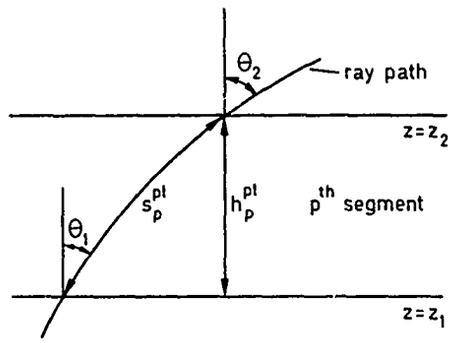

Figure 2. Ray parameters in planar propagation model

Segmentation is carried out in such a way that B" = constant per segment p (Figure 2). The ray parameters are functions of the refractive index profile and θ. In the planar model the ray parameters per segment become

- $h_{p_{p\ell}}$ = height difference of the ray = segment thickness
- $d_{p_{p\ell}}$ = horizontal distance of the ray along the earth surface
- $s_{p_{p\ell}}$ = path length of the ray
- $t_{p_{p\ell}}$ = path delay of the ray

If a ray reaches a maximum or minimum height within the segment an extra segment is introduced based on these heights. The whole radio path is described by summing the ray parameters. The appeal of the planar model is that analytical formulas of the of the ray parameters can be given.

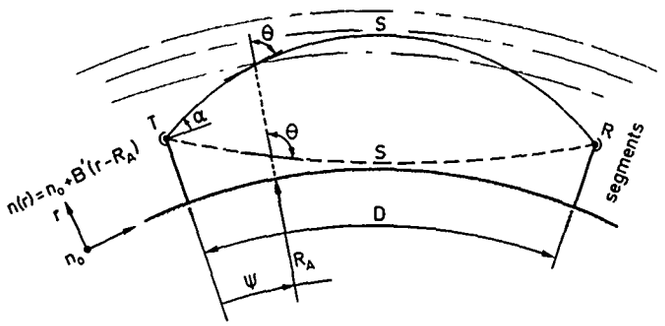

Figure 3. Spherical propagation model

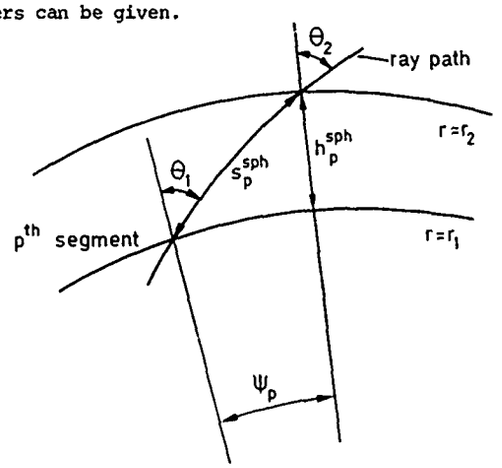

Figure 4. Ray parameters in spherical propagation model

In the model with spherical earth (Figure 3) the refractive index profile is characterized by the transformation

$$\frac{dn(r)}{dr} = \frac{dN(r_f)}{dr_f} - \frac{1}{R_a} + \frac{1}{R_f} = B' - \frac{1}{R_a} + \frac{1}{R_f}$$

where N = refractive index in the spherical model with arbitrary fictive radius R_f

B' = refractive index gradient per meter in the spherical model

Segmentation is illustrated in Figure 4 where B' = constant per segment p. The ray parameters in the spherical model become

- $h_{p_{sph}}$ = segment thickness
- $d_{p_{sph}} = R_f \cdot \psi_p$ = horizontal distance of the ray along the earth surface
- $s_{p_{sph}}$ = path length of the ray

- t_p^{sph} = path delay of the ray

Different analytical approximations for the ray parameters have been derived for $B' > -N(r_f)/r_f$, $B' < -N(r_f)/r_f$ and for the rays which reach maximum heights. Per segment analytical expressions can be obtained by making approximations in the ray theory, especially of the term

$$I = \sqrt{r_f^2 N^2(r_f) - C^2}$$

Using Snell's law for a spherical layered medium the ray path constant C becomes

$$C = N(r_f) \cdot r_f \cdot \sin\theta$$

For $B' < -N(r_f)/r_f$ the term I yields

$$I \approx \sqrt{(r_m^2 - r_f^2)K_p}$$

r_m is the maximum r_f value the ray would reach if the refractive index gradient B_p' = constant were extended to above. This means $r_m \geq r_2$. The factor K_p is chosen so that for $r_m > r_2$

$$(r_m^2 - r_2^2)\, K_p = r_2^2 N^2(r_2) - C^2$$

and for $r_m = r_2$

$$K_p = -N^2(r_1) - B_p' \cdot N(r_1) \cdot r_1$$

For $B' > -N'r_f)/r_f$ the term I yields

$$I \approx \sqrt{K_p'(r_f^2 - r_1^2) + K_p''}$$

K_p' and K_p'' are chosen so that the approximation is optimal for $r_f = r_1$; K_p' and K_p'' become

$$K_p' = N^2(r_1) + B_p' \cdot N(r_1) \cdot r_1$$

$$K_p'' = N^2(r_1) \cdot r_1^2 - C^2$$

3. Path delay computations and accuracy analysis

To make comparisons between planar and spherical models computer programs have been developed. The input parameters in the programs are

- link geometry (i.e. antenna heights, distance between antennas, earth radius)
- refractive index profiles linearized in a given number of segments
- elevation angles of transmitted rays

For an incoming ray at the aperture of the receiver antenna the results are

- path length and path delay τ
- angle of arrival α
- amplitude and phase

In case the elevation angles of transmitted and received rays are within 1 degree the main differences between the models are mostly found in path delay and amplitude computations. Therefore, in this section results of path delay computations are compared for the spherical model with $R_f = R_a$ and the planar model. For simplicity a constant refractive index gradient B' and thus a constant B" has been assumed over the atmospheric height region of interest. For the spherical model this height region is subdivided into seg-

ments with a constant thickness of 10 meters. The antenna heights at transmitter and receiver equals 100 m above the earth. Three different B' (and B") values are considered:

a. $B'_a = -5 * 10^{-7}$ $[m^{-1}]$ ⇒ $B''_a = -3.4 * 10^{-7}$ $[m^{-1}]$

b. $B'_b = -.78 * 10^{-7}$ $[m^{-1}]$ ⇒ $B''_b = .78 * 10^{-7}$ $[m^{-1}]$

c. $B'_c = 1 * 10^{-7}$ $[m^{-1}]$ ⇒ $B''_c = 2.6 * 10^{-7}$ $[m^{-1}]$

In these three cases the angle of arrival α dependency of the distance D is approximated by

a'. $D_a \approx 106 \cdot \alpha$ [km] α in degrees

b'. $D_b \approx 420 \cdot \alpha$ [km]

c'. $D_c \approx -135 \cdot \alpha$ [km]

The path delay computations $\Delta\tau = T_{total} - T_o$ for both models are shown in Figures 5-7 where:

- T_{total} = total path delay time from transmitting to receiving antenna
- T_o = delay time of a ray propagating at the earth's surface with a refractive index at earth $n_o = 1.0002$ and $B' = -1/R_a$

The figures give indication of larger $\Delta\tau$ values in the spherical model. By way of example, differences in $\Delta\tau$ up to 2.5 ns are found for angles less than 0.3 degrees and distances less than 40 km.

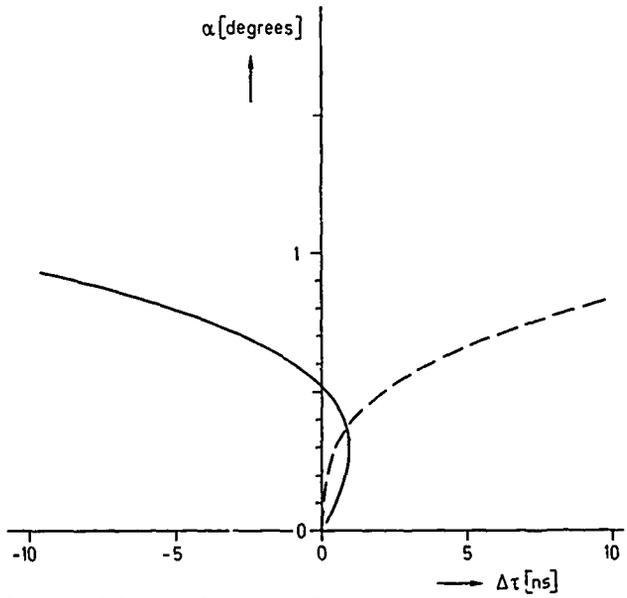

Figure 5. Path delay as function of α, for $B'_a = -5.0 * 10^{-7}$ $[m^{-1}]$ (solid line), and $B''_a = -3.4 * 10^{-7}$ $[m^{-1}]$ (dotted line)

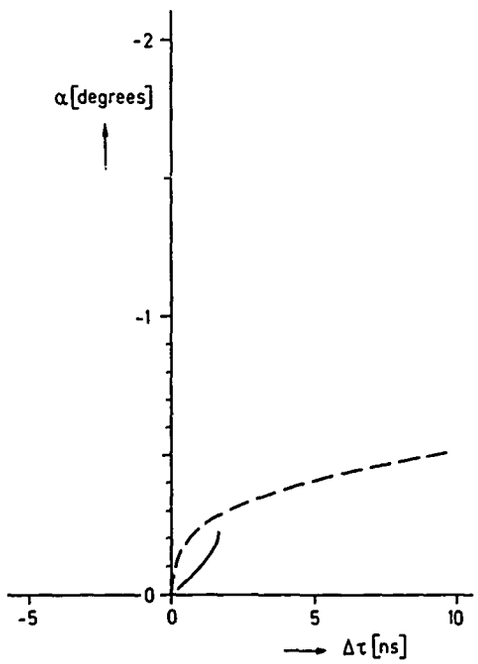

Figure 6. Path delay as function of α, for $B'_a = -.78 * 10^{-7}$ $[m^{-1}]$ (solid line), and $B''_a = .78 * 10^{-7}$ $[m^{-1}]$ (dotted line)

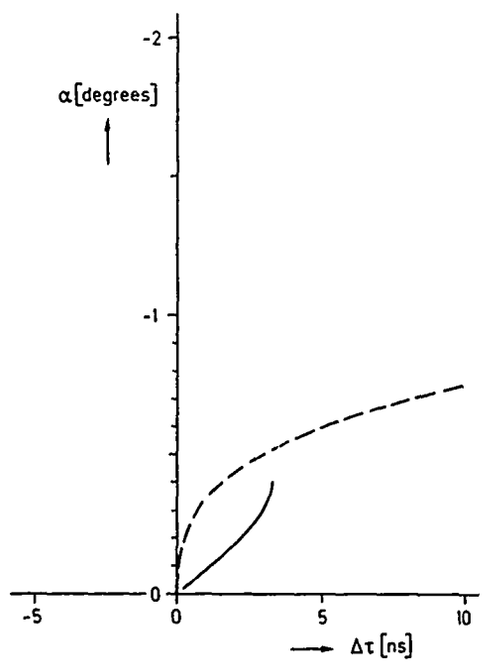

Figure 7. Path delay as function of α, for $B'_a = 1.0 * 10^{-7}$ $[m^{-1}]$ (solid line), and $B''_a = 2.6 * 10^{-7}$ $[m^{-1}]$ (dotted line)

To verify the convergence in the accuracy of the numerical computations for the spherical model $\Delta\tau$ computations have been made for specific angles and the number of segments (segment thicknesses which have been chosen are 10, 5, 1, and 0.25 meters) has been increased. In Figures 8 and 9 the accuracies are given

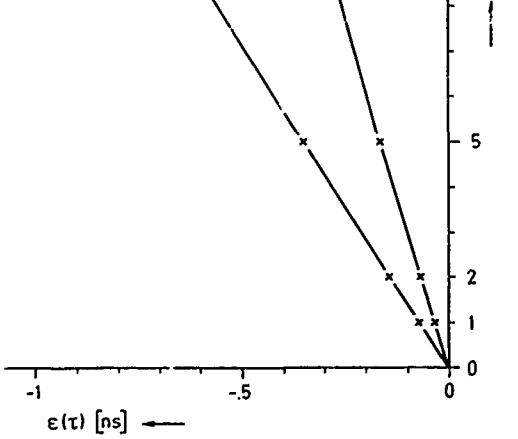

Figure 8. Error $\varepsilon(\tau)$ in $\Delta\tau$ computations as function of segment thickness d_s for $B' = -5.0 * 10^{-7}$ [m^{-1}]

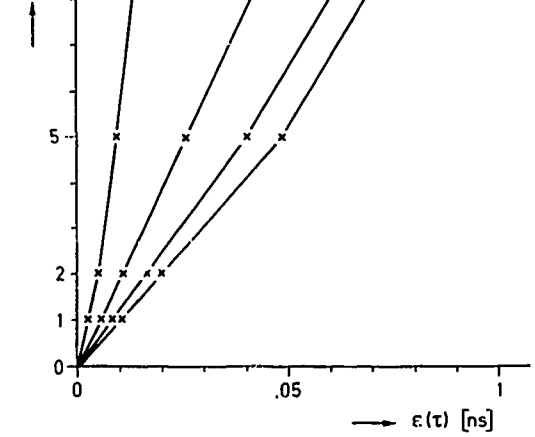

Figure 9. Error $\varepsilon(\tau)$ in $\Delta\tau$ computations as function of segment thickness d_s for $B' = 1.0 * 10^{-7}$ [m^{-1}]

for $B' = -5 \cdot 10^{-7}$ [m^{-1}] and $B' = 10^{-7}$ [m^{-1}]. The point of convergence in the origin has been obtained by extrapolation of the curve for a segment thickness of 1 m and a thickness of 0.25 m. From these results it can be seen that for segment thicknesses less than 10 meters the accuracy lies within 1 ns, which is less than the differences between the spherical and the planar model.

4. The modified logarithmic refractive index profile

An application of the theory is given for a refractive index profile characteristic of a duct above water. This model has been chosen because strong gradients and thus strong convergence or divergence of the rays can be expected just above the water surface. At the same time there is the possibility to investigate whether a simple relationship exists between the amplitude of incoming rays and their delay time.

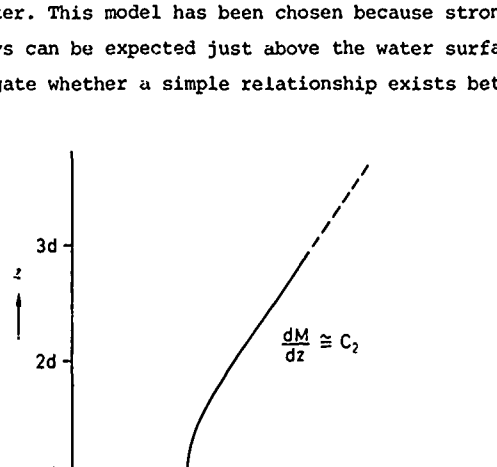

Figure 10. Modified logarithmic refractive index profile above a planar earth

For the microwave link the following is selected:

- distance between transmitter and receiver = 40 km
- antenna heights = 80 m

The modified logarithmic refractive index profile above a flattened earth is given by (Figure 10).

$$M(z) = C_2 \left[z - z_1 - (d + z_o) \cdot \ln\left(\frac{z+z_o}{z_1+z_o}\right) \right] + M_1$$

where

d = duct height (5 - 50 meters)

z_o = roughness parameter at the earth's surface (10^{-3} m)

z_1 = height where $M(z_1) = M_1$

and C_2 characterizes dM/dz at high altitudes ($z > 3d$).

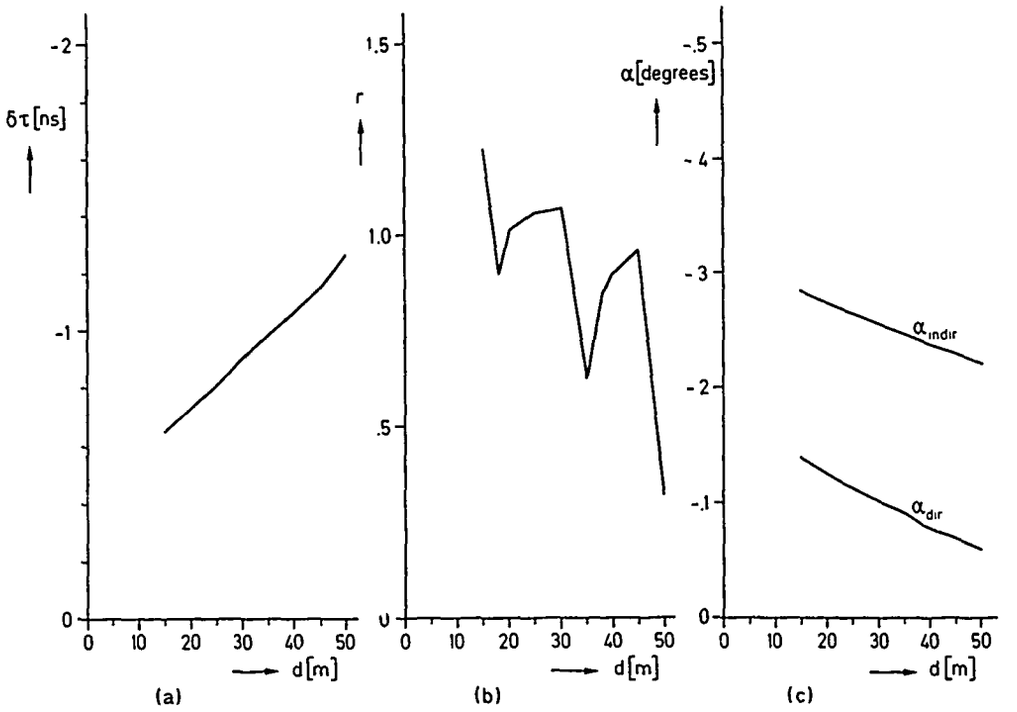

Figure 11. Computational results as function of duct height d.
Model 1: k = 1, M_1 = 325; a) time delay difference δτ; b) relative amplitude of the indirect ray; c) angles of arrival

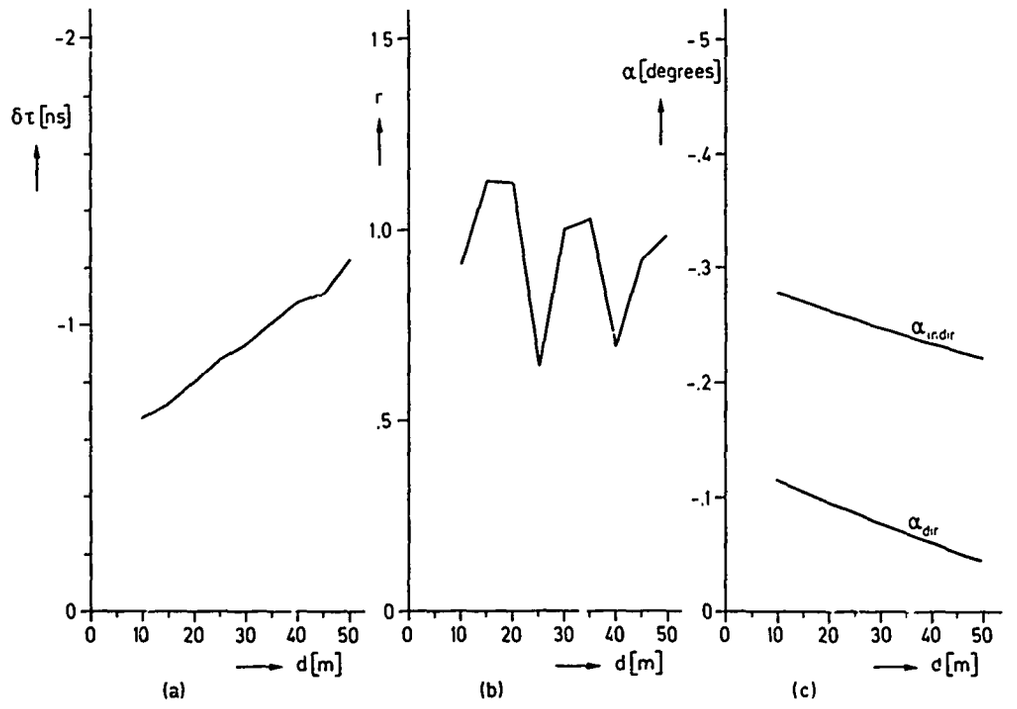

Figure 12. Computational results as function of duct height d.
Model 2: k = 4/3, M_1 = 325; a) time delay difference δτ; b) relative amplitude of the indirect ray; c) angles of arrival

The refractive index n above the spherical earth is determined by:

$$M(z) = (n - 1 + \frac{z}{R_a})\ 10^6 \Rightarrow dM/dz = (dn/dz + 1/R_a)\ 10^6$$

where dn/dz = refractive index gradient above a spherical earth with earth radius R_a.
For a fictive earth radius $R_f = kR_a$ it is found that:

$$R_f = \frac{1}{(dn/dz + 1/R_a)} \Rightarrow dM/dz = \frac{10^6}{kR_a} \simeq C_2 \qquad \text{for } z > 3d$$

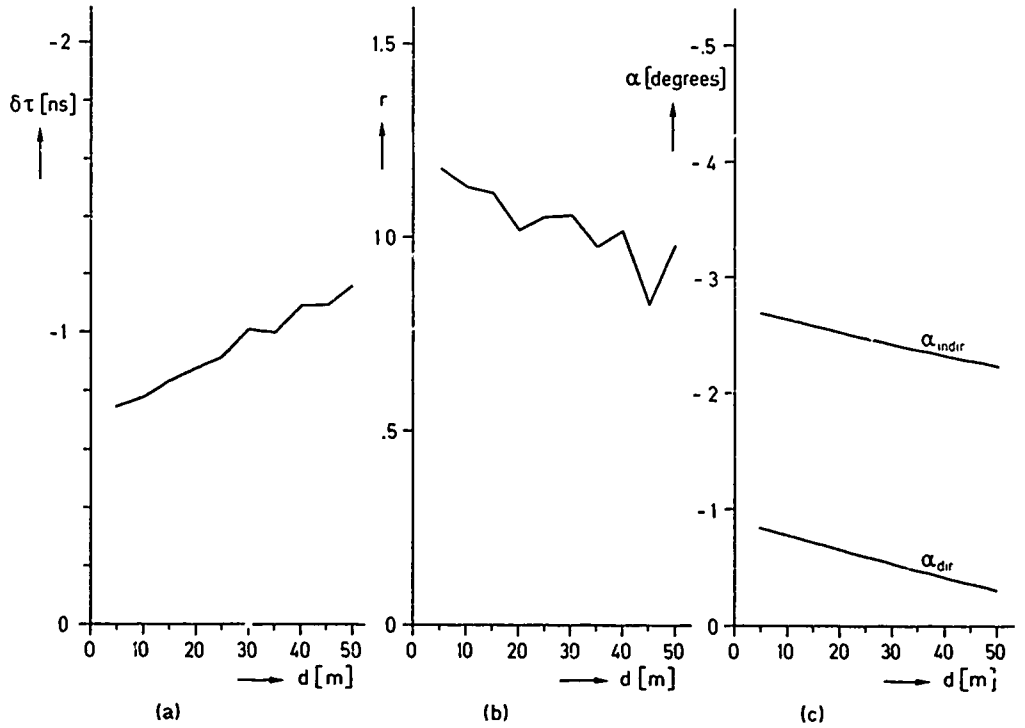

Figure 13. Computational results as function of duct height d;
Model 3: k = 2, M_1 = 325; a) time delay difference δτ; b) relative amplitude of the indirect ray; c) angles of arrival

This means that k determines the modelconditions for high altitudes. The computations with 1 meter segmentation and for k = 1, 4/3 (standard atmosphere above the duct) and k = 2, are presented in Figures 11, 12 and 13. In these figures δτ is the delay time difference and r is the relative amplitude factor of the two rays in this two-way propagation model.

A dominant k-dependency on δτ and a clear correlation between δτ and α are found as a function of the duct height, while no simple relationship exists between δτ and r. From Section 3 it is known that the appropriate spherical model has to be used for accurate δτ computations.

Conclusions

In this paper it is proposed that for path delay computations in multipath fading conditions spherical models be used. In the spherical model analytical formulas for the ray parameters have been used, assuming constant refractive index gradients per segment. By doing so the computing time can be reduced considerably relative to numerical solutions of the differential equations. The accuracy analysis shows strong convergence in path delay results by decreasing segment thicknesses. The example of a two-way spherical model based on surface duct layers above water indicates a strong relationship between time delay differences and angles of arrival combined with a dominant dependency of the model on the time delay computations.

Acknowledgements

Many thanks are due to the Dutch PTT, Dr. Neher Laboratory, for having made this study possible.

References

(1) K.P. Dombek: "Minderung von Mehrwegeschwund durch adaptive Schwenkung der Antennecharackteristik", NTG-Fachtagung, "Richtfunk" München 1980, NTG-Fachberichte Band 70, VDE-Verlag, GmbH, Berlin, pp. 133-138

(2) L.P. Ligthart, K.P. Dombek, G. Doro, V. Santomaa: "COST-204 review on limited scan arrays", paper presented at the joint ESA/COST 204 Phased-Array Antenna Workshop, held at ESTEC, Noordwijk, The Netherlands, 13 June 1983, ESA SP-204, pp. 15-21

DISCUSSION

M.P.M. Hall (U.K.): Your Figures 1-4 show a rather simple case where both transmitter and receiver are situated at a height above which the refractive index decreases sharply with height, and below which it increases sharply with height. Could you please comment on how the main conclusions of your paper would be different for a more general ducting geometry in which the terminal height would not be at this region of refractive index change, and where the curvature of each ray would change significantly with height and even change direction along its path?

L.P. Ligthart (The Netherlands): In the spherical model, arbitrary refractive index profiles may be used and antenna heights may vary. Maximum time differences $\Delta\tau$ occur in the case you mentioned and are shown in Figures 1-4. The main conclusion remains, as can be seen from Figures 11-13 in which a modified logarithmic refractive index profile has been taken.

U. Buse (Germany): At which frequency range are your models valid?

L.P.Ligthart (The Netherlands): At 4 and 6 GHz.

S. Rotheram (U.K.): The use of a flat earth with an earth flattening transformation and a modified refractive index should give the same answer as a spherical earth and the ordinary refractive index. In two dimensions (cylindrical geometry) the earth flattening transformation can be made exact.

L.P. Ligthart (The Netherlands): The earth flattening transformation yields a modified refractive index, which gives approximate results. In the limit of small elevation angles, exact results are obtained. In comparison between planer and spherical propagation models, differences have been found only in the path delay.

L. Boithias (France): Vous ne tenez pas compte des variations horizontales de l'indice de réfraction. Les erreurs introduites ainsi ne sont-elles pas supérieures à celles que vous envisagez de corriger?

L.P. Ligthart (The Netherlands): Horizontal variations in the refractive index can influence the numerical results. Therefore experimental verification of the models is needed.

T.A.Th. Spoelstra (The Netherlands): This is a comment. The necessity to use a planar or spherical earth approximation in the model depends on the accuracy one needs. In radio astronomy, correlation of signals from telescopes at distances of a few hundred meters make a spherical approximation mandatory. Furthermore it should be valid for all elevation angles.

N. Amitay (U.S.): Roughly, what improvement can you expect to obtain by using angular diversity?

L.P. Ligthart (The Netherlands): Deep fadings can be reduced between 5 to 10 dB by using angular diversity. The effects on group delay depends on delay time differences.